Cancer Biol Med 2026. doi: 10.20892/j.issn.2095-3941.2025.0326

ORIGINAL ARTICLE

Antitumor effects of STING agonists on nervous system tumors *via* tumor-intrinsic STING-STAT1-mediated HMGN2 expression

Zijian Lv[1]*, Tiance Wang[1]*, Runjia Fan[1]*, Qianyi Ming[1]*, Jiejie Liu[1], Yulin Jia[1], Yan Zhang[1], Meixia Chen[1], Wei Chen[2], Zhengfan Jiang[3], Weidong Han[1,4], Qian Mei[1]

[1]Department of Bio-Therapeutic, The First Medical Center, Chinese PLA General Hospital, Beijing 100853, China; [2]Department of Pathology, The Fifth Medical Center, Chinese PLA General Hospital, Beijing 100853, China; [3]Key Laboratory of Cell Proliferation and Differentiation of the Ministry of Education, School of Life Sciences, Peking University, Beijing 100871, China; [4]Changping Laboratory, Beijing 102206, China

ABSTRACT

Objective: Clinical use of stimulator of interferon genes (STING) agonists has challenges due to poor responsiveness and variable efficacy. Therefore, identifying tumor types that are sensitive to these agents and clarifying the underlying mechanisms are essential.

Methods: *In vitro* screening was performed to identify tumor types that are sensitive to STING agonists. The non-nucleotide agonist, SR-717, and the macrocyclic agonist, E7766, were compared for efficacy. Complementary *in vivo* and *in vitro* studies, including gene-knockout models, HMGN2-knockout Neuro-2A and CT-2A cells apoptosis assays, and murine tumor models, were then performed. These experiments focused on the mechanism by which SR-717 mediates antitumor effects and emphasized the role of STING signaling-induced high-mobility group nucleosome-binding protein 2 (HMGN2). In addition, the potential of HMGN2 as a prognostic biomarker was assessed.

Results: Neuroblastomas and glioblastomas, two nervous system tumors, were shown to be sensitive to STING agonists. SR-717 exhibited greater antitumor efficacy compared to E7766. Mechanistic studies indicated that STING agonists promote apoptosis through activation of the intrinsic STING-signal transducer and activator of transcription 1 (STAT1)-HMGN2 axis within tumor cells. Ectopic expression of HMGN2 in melanoma cells, which naturally lack HMGN2, led to significant apoptosis. Furthermore, analysis of The Cancer Genome Atlas and Gene Expression Omnibus databases revealed positive correlation between elevated HMGN2 expression and patient survival, supporting the utility of HMGN2 as a prognostic biomarker.

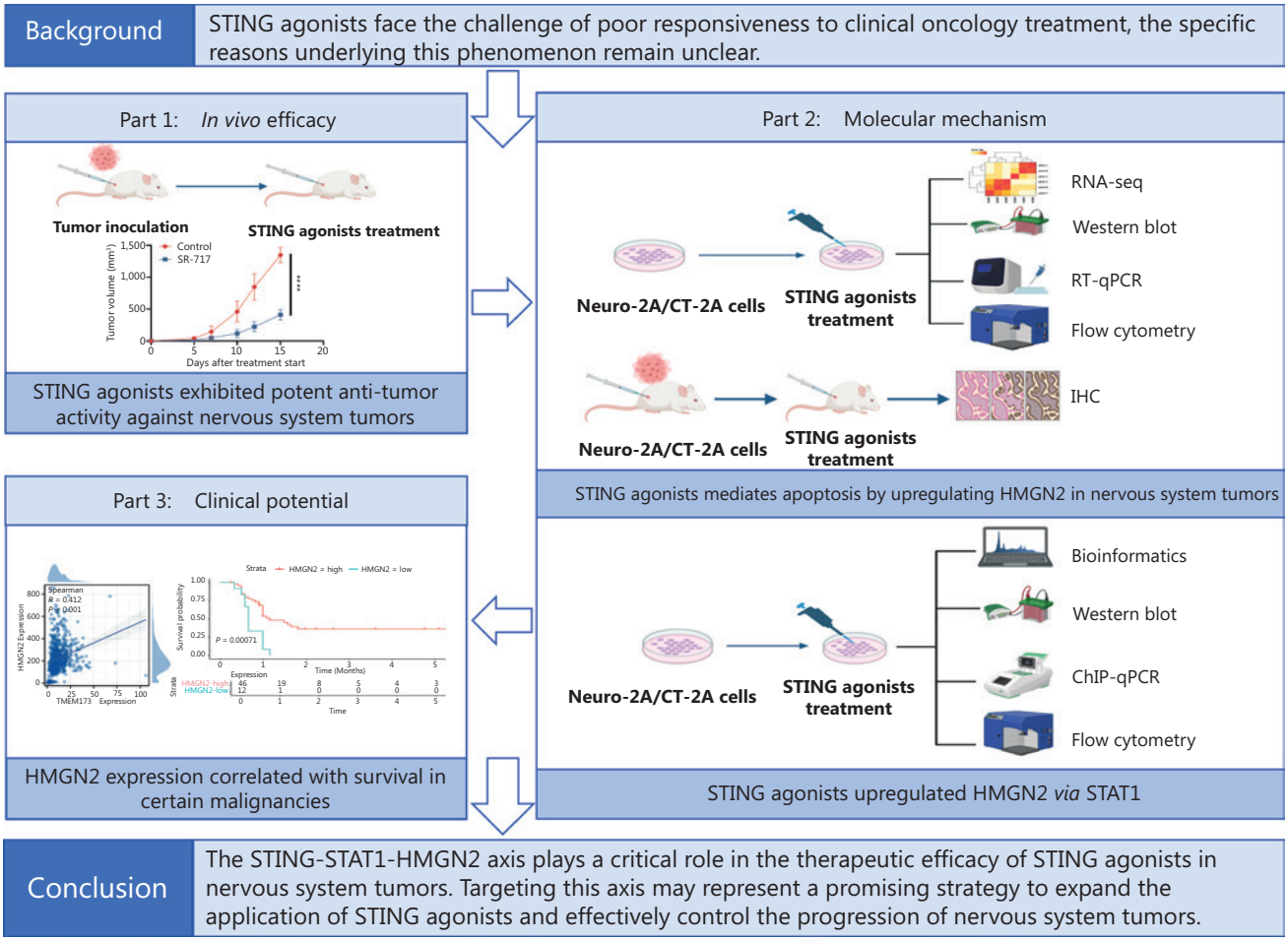
Conclusions: This study clarified the mechanism underlying the potent antitumor activity of SR-717 in nervous system tumors through activation of the STING-STAT1-HMGN2 signaling pathway and demonstrated that SR-717 has superior efficacy compared to E7766. In addition, HMGN2 was shown to exhibit translational potential as a prognostic biomarker for patient survival.

KEYWORDS STING agonists; SR-717; tumor immunity; HMGN2; biomarker

Introduction

The rapid advances in immunotherapy in recent years have attracted growing research interest in the regulatory mechanisms underlying innate immunity[1]. Among these mechanisms, the cyclic GMP-AMP synthase (cGAS)-stimulator of interferon genes (STING) signaling pathway has emerged as a pivotal cascade in innate immune modulation[2-4]. Activation of the cGAS-STING pathway triggers the robust induction of type I interferons (IFNs) and initiates a coordinated release of pro-inflammatory cytokines and chemokines[5-9]. These factors enhance the functionality of immune cells, including dendritic cells (DCs) and T lymphocytes[10-14]. Emerging evidence highlights tumor cell-intrinsic roles associated with STING activation. Endogenous stimulation of this pathway induces autophagy, suppresses tumor progression, and inhibits metastasis, consequently prolonging survival in murine tumor models[15]. These multifaceted immunomodulatory and direct antitumor properties suggest STING agonists as promising therapeutic candidates for cancer treatment[16].

*These authors contributed equally to this work.
Correspondence to: Zhengfan Jiang, Weidong Han and Qian Mei
E-mail: jiangzf@pku.edu.cn, hanwdrsw@163.com and meiqnn@hotmail.com
ORCID ID: https://orcid.org/0000-0002-1247-1382, https://orcid.org/0000-0003-3207-3899 and https://orcid.org/0009-0006-9605-5293
Received June 17, 2025; accepted October 30, 2025.
Available at www.cancerbiomed.org
©2026 The Authors. Creative Commons Attribution-NonCommercial 4.0 International License (CC BY-NC 4.0)



Study flow Antitumor effects of STING agonists on nervous system tumors *via* tumor-intrinsic STING/STAT1-mediated HMGN2 expression. **Part 1** shows that STING agonists exert significant inhibitory effect on the progression of nervous system tumors after *in vitro* screening of various tumors and subsequent *in vivo* validation. **Part 2** shows that treatment with STING agonists activates the endogenous STING signaling in nervous system tumors, promotes the phosphorylation of the downstream transcription factor STAT1, and upregulates the intracellular expression of HMGN2 in tumor cells. Furthermore, overexpression of HMGN2 activates the intrinsic apoptotic pathway, thereby inducing tumor cell apoptosis. **Part 3** shows that high expression of HMGN2 in a variety of human malignant tumors can effectively prolong patient survival, which highlights the therapeutic potential of STING agonists targeting HMGN2. ***, $P < 0.001$; STING, stimulator of interferon genes; HMGN2, high-mobility group nucleosome-binding domain 2; STAT1, signal transducer and activator of transcription 1.

Despite promising preclinical efficacy, a significant gap exist between the anticipated potential and actual clinical outcomes of STING agonists[17-19]. Notably, inter- and intra-tumoral heterogeneity may substantially contribute to this discrepancy[20,21]. However, previous studies have predominantly focused on STING agonist-mediated immunomodulation within the tumor microenvironment, largely neglecting the intrinsic regulatory effects on tumor cells[22-24]. Although preclinical studies have confirmed that STING agonists effectively control glioblastoma and neuroblastoma progression in mouse models by remodeling the immune microenvironment and inducing NOD-like receptor thermal protein domain associated protein 3 (NLRP3) inflammasome-mediated pyroptosis[25-27], clinical trials targeting nervous system tumors are lacking. Currently, there is a lack of clinical trial data supporting the safety and efficacy of STING agonists, as well as evidence clearly identifying which patients may benefit from STING agonist treatment. Therefore, clarifying tumor cell-intrinsic STING activation mechanisms and identifying molecular characteristics of STING-sensitive tumors are key to advancing clinical translation in nervous system tumors.

HMGN2 is a member of the high-mobility group nucleosome-binding (HMGN) protein family, which consists of five members (HMGN1, HMGN2, HMGN3, HMGN4, and HMGN5)[28]. Accumulating evidence indicates that HMGN2 functions as a tumor suppressor in several cancers. For example, overexpression of HMGN2 in hepatocellular carcinoma

results in reduced proliferation and enhanced apoptosis[29]. In addition to cell-intrinsic roles, HMGN2 also functions as an extracellular antitumor effector molecule secreted by activated $CD8^+$ T cells, through which HMGN2 is translocated into tumor cells and mediates dose-dependent tumor-killing effects[30]. These findings collectively suggest that HMGN2 exhibits broad antitumor activities across various cancers. However, the precise mechanisms underlying its antitumor effects are complex and warrant further investigation.

This study demonstrated that SR-717, a STING agonist, exhibits distinctive and potent antitumor efficacy against nervous system tumors. Further analysis revealed that this efficacy primarily resulted from the direct effects of the STING agonist on tumor cells. SR-717 activates the intrinsic STING/STAT1 pathway within nervous system tumor cells, thereby increasing HMGN2 expression, promoting apoptosis, and inhibiting tumor growth. Clinical data analysis also indicated a strong correlation between HMGN2 expression and STING pathway activity with elevated HMGN2 levels corresponding to improved patient prognosis. Collectively, these findings offer novel insights into the mechanisms underlying STING agonist therapy for nervous system tumors.

Materials and methods

Mice

Specific pathogen-free (SPF) A/J, C57BL/6J, $Rag^{-/-}$, and NSG mice, 4–6 weeks old and weighing 24–26 g, were purchased from SPF (Beijing) Biotechnology Co., Ltd. [License No.: SCXK (Beijing) 2016-0002]. Animal experiments were approved by the Animal Ethics Committee of the General Hospital of the Chinese People's Liberation Army. Breeding and experimental conditions complied with relevant national regulations regarding animal experimentation, health inspections, and quarantine.

Cells and cell culture

CT-26, MC38, Neuro-2A, CT-2A, 4T1, B16f10, and LLC tumor cells were obtained from the American Type Culture Collection [ATCC] (Manassas, VA, USA). Cells were cultured in DMEM (Gibco, Thermo Fisher Scientific, Waltham, MA, USA) or RPMI-1640 medium (Gibco) supplemented with 10% fetal bovine serum [FBS] (Gibco), 100 U/mL penicillin (MCE, Shanghai, China), and 100 mg/mL streptomycin (MCE). All cell cultures were free from contamination by the operator.

Subcutaneous tumor model in mice

Neuro-2A, CT-2A, and B16F10 cells (2×10^5 or 5×10^5 cells/100 μL of PBS) were subcutaneously injected into the abdomen of A/J, C57BL/6, $Rag^{-/-}$, or NSG mice. Treatment with 30 mg/kg of SR-717 or 4 mg/kg of E7766 began 6 d after tumor cell injection, as illustrated in **Figures S1F and S2H**.

STING agonists

SR-717 (HY-131454; MCE, Shanghai, China) was used at a concentration of 10 μM (Neuro-2A, IC_{50} = 11.64 μM; and CT-2A, IC_{50} = 10.2 μM; **Figure S1A, B**)[31] for *in vivo* experiments, and administered at a dose of 30 mg/kg[32] for *in vivo* studies.

E7766 (HY-111999A; MCE) was used at a concentration of 4.9 μM for *in vitro* studies and at a dose of 4 mg/kg for *in vivo* studies[33].

Apoptosis assay

Tumor cells were seeded in 6-well plates and incubated overnight to allow attachment. The medium was then replaced with complete culture medium containing 10 μM SR-717 or 4.9 μM E7766. After 48 h of culture, cells were collected by trypsinization and stained using an Annexin V-FITC staining kit (BioLegend, San Diego, CA, USA). Apoptotic cells (FITC-positive) were quantified by flow cytometry.

Quantitative RT-qPCR

Total RNA was extracted using TRIzol reagent (Thermo Fisher Scientific, Waltham, MA, USA). Reverse transcription was performed using ReverTra Ace qPCR RT Master Mix (Toyobo, Osaka, Japan), following the manufacturer's instructions. qPCR was performed using SYBR Green Real-time PCR Master Mix (Toyobo) on a 7500 Fast Real-Time PCR system with a 96-well block (Applied Biosystems, Waltham, MA, USA). Data were normalized to *GAPDH* expression. The primer sequences are listed in **Table S1**.

Western blot

Cells were rinsed twice with ice-cold PBS and lysed using RIPA buffer (YangGuangBio, Beijing, China) containing protease inhibitors (MCE, Shanghai, China). Protein concentrations in the lysates were measured using the bicinchoninic acid assay and adjusted with extraction reagent. Western blotting was performed using the antibodies listed in **Table S2**. Band intensity was analyzed using ImageJ software (NIH, Bethesda, MD, USA) and normalized to GAPDH.

Immunohistochemistry (IHC)

Tumor tissues were fixed, dehydrated, embedded in paraffin, and sectioned. Sections were incubated overnight at 4°C with primary antibody against HMGN2 (10953-1-AP; Proteintech, Wuhan, China). Sections were then incubated with horseradish peroxidase (HRP)-conjugated goat anti-rabbit IgG for 2 h,

followed by visualization with Diaminobenzidine [DAB]. Hematoxylin counterstaining was performed for 1 min. Immunohistochemical staining and histopathologic assessments were analyzed under a microscope.

RNA sequencing

Neuro-2A and CT-2A cells were treated with 10 μM SR-717 for 48 h. Total RNA was extracted using TRIzol reagent (T9424; Sigma, St. Louis, MO, USA). RNA sequencing and data analysis were performed by Novogene (Shanghai, China). Gene Ontology (GO) and differential gene expression analyses were performed.

Cell Counting Kit-8 (CCK-8)

Cell viability was measured using the CCK-8 assay (Vazyme, Nanjing, China). Cell suspensions were seeded into 96-well flat-bottomed plates (Vazyme). After treatment with 10 μM SR-717 for 48 h at 37°C in 5% CO_2, 10 μL of CCK-8 solution was added and incubated for an additional 3 h. Absorbance was measured at 450 nm using a microplate reader (Thermo Fisher Scientific, Waltham, MA, USA).

RNA interference

Murine STING, STAT1, and control small-interfering RNAs (siRNAs) were obtained from Genomeditech (Shanghai, China). Cells were transfected with 50 pmol/mL of siRNA oligonucleotides using Lipofectamine 3000 (Invitrogen, Waltham, MA, USA). The primer sequences are provided in **Table S3**.

HMGN2 knockout (KO) cell lines

Murine Neuro-2A and CT-2A cells underwent HMGN2 KO using the Lonza 4D-Nucleofector™ kit (VCA-1003; Lonza, Basel, CH). Briefly, 5×10^5 cells were harvested, washed twice with PBS, and resuspended in electroporation buffer containing 2 μg of Cas9 protein and 2 μg of HMGN2 single-guide RNA (sgRNA). Electroporation was performed using the EO-137 program (Lonza) following the manufacturer's instructions. The cells were transferred to pre-warmed complete medium immediately after electroporation. KO efficiency was verified by western blot 4 d post-electroporation. The sgRNA sequence targeting mouse HMGN2 was GGGGAAAGCTGACGCCGGGA.

Overexpression of HMGN2

HEK293T cells were seeded in 75 cm^2 flasks (Vazyme, Nanjing, China) and transfected with 10 μg of lentiviral vectors (Genomeditech Shanghai, China) encoding HMGN2 or GFP (negative control) to establish stable HMGN2-overexpressing cell lines. The medium was replaced after 48 h and viral supernatants were collected and filtered through 0.45-μm syringe filters (Millipore, Billerica, MA, USA). Neuro-2A, CT-2A, and B16F10 cells were incubated with lentiviral supernatants for 24 h and selected using 2 μg/mL of puromycin (Sigma) according to the manufacturer's protocol. Cells transduced with the HMGN2 lentivirus were designated the HMGN2-OE group, cells transduced with GFP lentivirus served as the vehicle group, and untreated cells served as the control group.

Chromatin immunoprecipitation-quantitative PCR (ChIP-qPCR)

Neuro-2A and CT-2A cells were processed using the Simple ChIP® Plus Sonication Chromatin IP kit (56,383; CST, Danvers, MA, USA). Chromatin was incubated overnight at 4°C with anti-STAT1 antibody (CST), while normal IgG antibody (CST) served as the negative control. RT-PCR analysis was performed as previously described. The primer sequences are listed in **Table S4**.

Prognostic analysis of HMGN2

The bulk RNA-seq data and clinical information of patients in this study were sourced from The Cancer Genome Atlas Colon Adenocarcinoma (TCGA-COAD), TCGA-kidney renal clear cell carcinoma (KIRC), TCGA-glioblastoma multiforme (GBM), TCGA-cervical squamous cell carcinoma and endocervical adenocarcinoma (CESC), and TCGA-pancreatic adenocarcinoma (PAAD) cohorts, which include 254 cases of colon cancer, 521 cases of clear cell renal cell carcinoma, 58 cases of glioblastoma, 283 cases of cervical cancer, and 176 cases of pancreatic cancer. The data were downloaded using the TCGA biolinks R package and normalized to transcripts per million (TPM). The TPM data were log2-transformed before proceeding with further analysis to enhance the statistical stability of the data and reduce the uneven variance. The GSE49710 dataset from the Gene Expression Omnibus (GEO) database was included for subsequent analysis due to the lack of sequencing data for neuroblastoma in the TCGA database. GSE49710 contains microarray data and clinical information for 498 neuroblastoma cases with gene annotations based on the GPL16876 platform. Batch correction was performed using the normalizeBetweenArrays from the limma R package (url) to ensure the reliability and comparability of the experimental results before further analysis, given the potential batch effects between samples that could lead to systematic differences.

Survival analysis was performed using the survival R package (url); the survfit function was used to model Kaplan–Meier survival curves. The surv_cutpoint function from the

survminer package was used to automatically select the optimal cut-off value by maximizing the log-rank test statistic, dividing continuous variables into two groups to determine the best threshold for survival data grouping comparisons.

All the above analyses were performed using R software (version 4.4.1).

Statistical analysis

Data are presented as the mean ± standard error of the mean. Statistical analyses were performed using GraphPad Prism (version 10.0; GraphPad Software, San Diego, CA, USA). Survival analyses were performed using the survival package in R software (version 4.4.1). An unpaired two-tailed Student's t-test or one-way ANOVA with the Bonferroni multiple comparison correction or one-way ANOVA with Tukey's honestly significant difference test for multiple comparisons were applied for normally distributed data. The Wilcoxon matched-pairs signed-rank test for paired comparisons or the Kruskal–Wallis test for multiple groups was utilized for non-normally distributed data. Tumor growth was analyzed using repeated-measures ANOVA. The Spearman's correlation test was used to determine correlations.

Results

STING agonists exhibit potent antitumor activity against nervous system tumors

Drug sensitivity assays were performed using SR-717, a potent non-nucleotide small-molecule STING agonist, and E7766, a macrocyclic-bridged STING agonist, on 6 tumor cell lines, including Neuro-2A (neuroblastoma) and CT-2A (glioblastoma), to identify tumor types sensitive to STING agonists. CCK-8 cell proliferation assays showed significant suppression of Neuro-2A and CT-2A cell proliferation following 48 h of continuous exposure (**Figure 1A**). In contrast, the remaining four tumor lines, including colorectal cancer CT-26, exhibited no significant cytotoxicity (**Figure S1C**). These findings indicate intrinsic sensitivity of neural-origin tumors to STING pathway activation.

Apoptosis assays performed after a 48-h exposure to SR-717 or E7766 showed that both agonists effectively induced apoptosis in Neuro-2A and CT-2A cells (**Figures 1B and S1D**). Similar results were confirmed in human Neuroblastoma (NB) SH-SY5Y and Glioblastoma (GB) U87 cell lines (**Figure S1E**). Murine tumor models using were established *via* subcutaneous injection of Neuro-2A and CT-2A cells into the inguinal region of A/J and C57BL/6 mice to evaluate direct antitumor activity *in vivo* (**Figure S1F**). SR-717 intratumoral injections started on day 6 after implantation and continued every 3 d for 3 cycles. This regimen resulted in significant tumor suppression (**Figure S1G**).

Experiments were performed using $Rag^{-/-}$ mice deficient in T and B cells (**Figure S1H**) and NSG mice deficient in T, B, and NK cells (**Figure 1C**) to determine whether the antitumor activity of STING agonists requires immune cells. SR-717 maintained antitumor activity in both nervous system tumor models under severe immunodeficiency conditions, although efficacy was reduced compared to immunocompetent hosts. Treatment of tumor-bearing NSG mice with E7766 also effectively suppressed tumor growth, although to a lesser extent compared to SR-717 (**Figure S2A**).

Collectively, STING agonists demonstrated significant antitumor capabilities in tumors derived from the nervous system and the activity partially occurred independent of immune cells.

STING agonists mediate apoptosis in nervous system tumors *via* HMGN2 upregulation

RNA sequencing analysis was performed on Neuro-2A and CT-2A cells treated with SR-717 for 48 h to clarify the molecular mechanisms responsible for reduced tumor cell viability. This analysis aimed to identify common gene expression changes following STING pathway activation. Differential gene expression analysis revealed 80 shared genes significantly upregulated in SR-717-treated cells compared to controls. Annotation of the top 20 significantly upregulated genes identified *HMGN2* as a candidate gene of interest (**Figure 1D**). *HMGN2* was prioritized due to pronounced upregulation and an established apoptotic role in tongue squamous cell carcinoma[30]. We therefore hypothesized that HMGN2 mediates the antiproliferative effects of SR-717 on Neuro-2A and CT-2A cells.

Experiments were performed to confirm whether STING activation increases *HMGN2* expression in Neuro-2A and CT-2A cells. RT-qPCR (**Figures 1E and S2B**) and western blotting (**Figures 1F and S2C**) demonstrated that treatment with SR-717 or E7766 significantly upregulated *HMGN2* expression at the mRNA and protein levels. These results suggested that increased *HMGN2* expression is a common response to STING activation.

Additional experiments were performed to confirm whether apoptosis induced by STING agonists in nervous system tumor cells is mediated by HMGN2. First, stable HMGN2-overexpressing cell lines were established and transfection efficiency was verified by western blot analysis after 48 h (**Figure S2D**). Both SR-717 treatment and plasmid-driven HMGN2 overexpression significantly increased apoptosis in Neuro-2A and CT-2A cells (**Figure 2A, B**). Conversely, STING agonists failed to induce apoptosis effectively when HMGN2 was knocked out (**Figures S2E and 2C,D**). Re-expression of HMGN2 restored sensitivity to STING agonists (**Figures S2F and 2E, F**). Further analysis showed that HMGN2 overexpression induced apoptosis *via* enhanced cleavage of caspase-3 (**Figure S2G**).

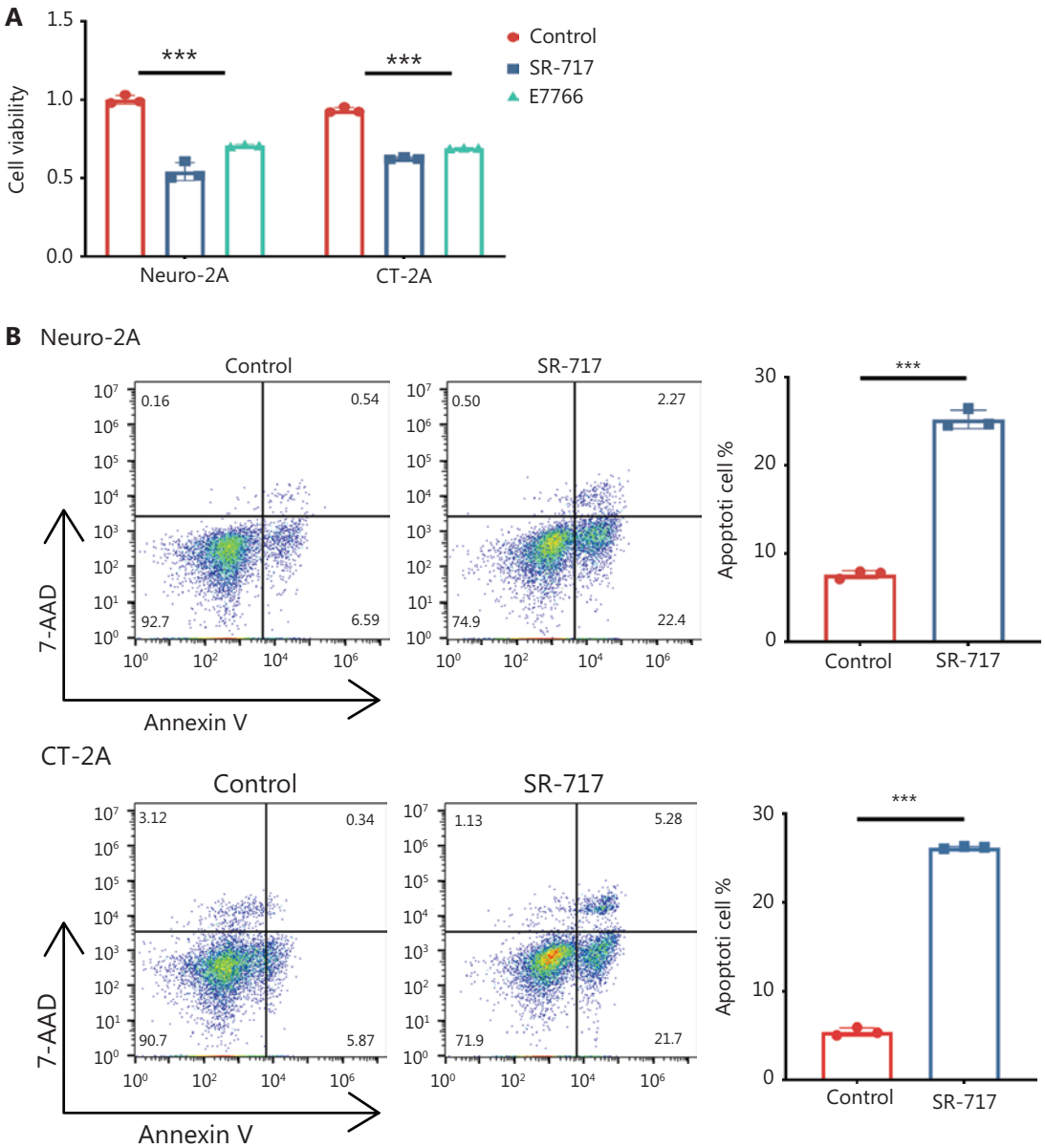


Figure 1 Continued

NSG mouse models bearing HMGN2-KO Neuro-2A and CT-2A tumors were established to verify these findings *in vivo* (**Figure S2H**). IHC staining of tumor tissues confirmed that STING agonists exert a stable regulatory effect on intratumoral HMGN2 in mouse tumor models (**Figure S2I**). HMGN2 deletion significantly impaired the tumor growth inhibition induced by STING agonists, which was consistent with the *in vitro* results (**Figures 2G,H and S3A–F**). However, restoring HMGN2 expression reinstated the antitumor effects of STING agonists (**Figures 2I and S3G–I**).

In conclusion, STING agonists activated the STING signaling pathway in neural tumor cells, resulting in increased HMGN2 expression, subsequent apoptosis, and inhibition of tumor progression.

HMGN2 has a crucial role in the antitumor effects of STING agonists

Additional tumor cell lines were treated with SR-717 to further confirm the role of HMGN2 in STING agonist-mediated tumor suppression. The untreated-Neuro-2A cells served as the control group, while non-small cell lung cancer exhibited high basal HMGN2 expression. Murine melanoma B16F10

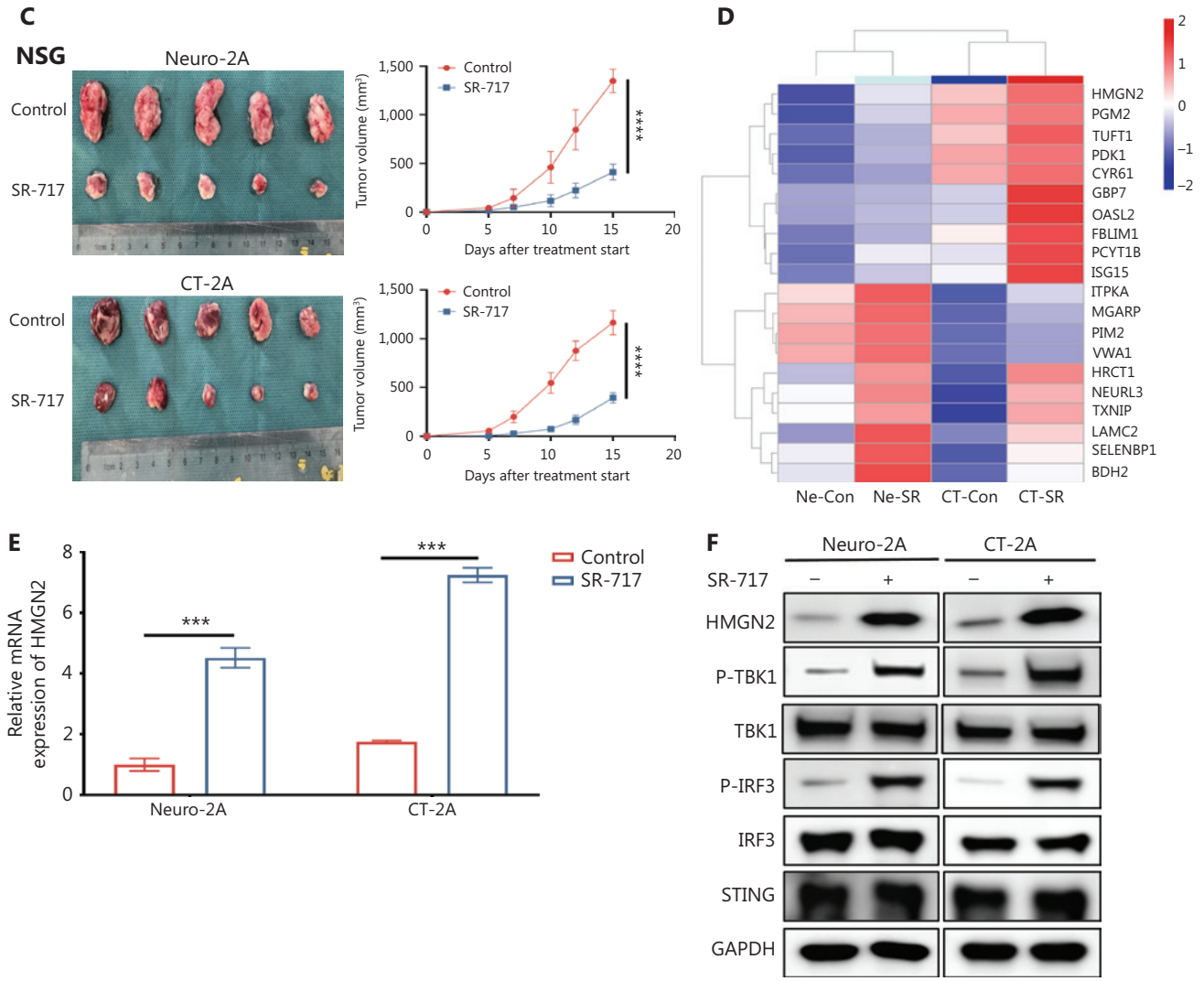


Figure 1 STING agonists exhibited potent antitumor activity against nervous system tumors. (A) The CCK-8 assay determined the effect of 10 μM SR-717 or 4.9 μM E7766 treatment for 48 h on viability of Neuro-2A and CT-2A cells. (B) FACS analysis of apoptosis levels in Neuro-2A and CT-2A cells in the control and SR-717 groups. (C) Images of tumors in the Neuro-2A and CT-2A cell subcutaneous models; quantification of tumor volume on the indicated days after the mice were treated with SR-717 at a dose of 30 mg/kg (n = 5). (D) Genes that were upregulated in the CT-2A- and Neuro-2A SR-717-treated groups (n = 80) were selected and the top 20 were chosen for presentation (|log 2FC| ≥ 1, P < 0.05). (E) RT-qPCR analysis of *HMGN2* gene mRNA levels in Neuro-2A and CT-2A cells after SR-717 treatment. (F) Western blot of STING pathway and HMGN2 expression in Neuro-2A and CT-2A cells upon SR-717 treatment. The bars represent the mean ± S.D. of 3 replicates (***P < 0.001, ****P < 0.0001, as determined by ANOVA with Tukey's honestly significant difference test for multiple comparisons). Control group was untreated, SR-717 group was treated with SR-717, E7766 group was treated with E7766.

cells showed minimal basal HMGN2 expression. Notably, SR-717 treatment did not significantly alter HMGN2 levels in LLC or B16F10 cells (**Figure 3A**). Western blot analysis confirmed low basal expression of HMGN2 in B16F10 cells, characterizing B16F10 cells as an HMGN2-deficient cell line (**Figure 3B**).

Flow cytometry analysis showed that SR-717 treatment did not induce apoptosis in LLC and B16F10 cells, which was consistent with the HMGN2 expression profiles (**Figure 3C**). NSG mice bearing B16F10 tumors were treated with SR-717 for three cycles to validate this observation *in vivo*. As hypothesized, no significant differences in tumor growth occurred between the treatment and control groups under the condition of HMGN2 deficiency (**Figure 3D**). HMGN2-overexpressing B16F10 cells were generated to clarify the underlying mechanism and transfection efficiency was confirmed by RT-qPCR and western blot (**Figure 3E, F**). Flow cytometry confirmed that ectopic HMGN2 expression strongly induced apoptosis in these cells (**Figure 3G**).

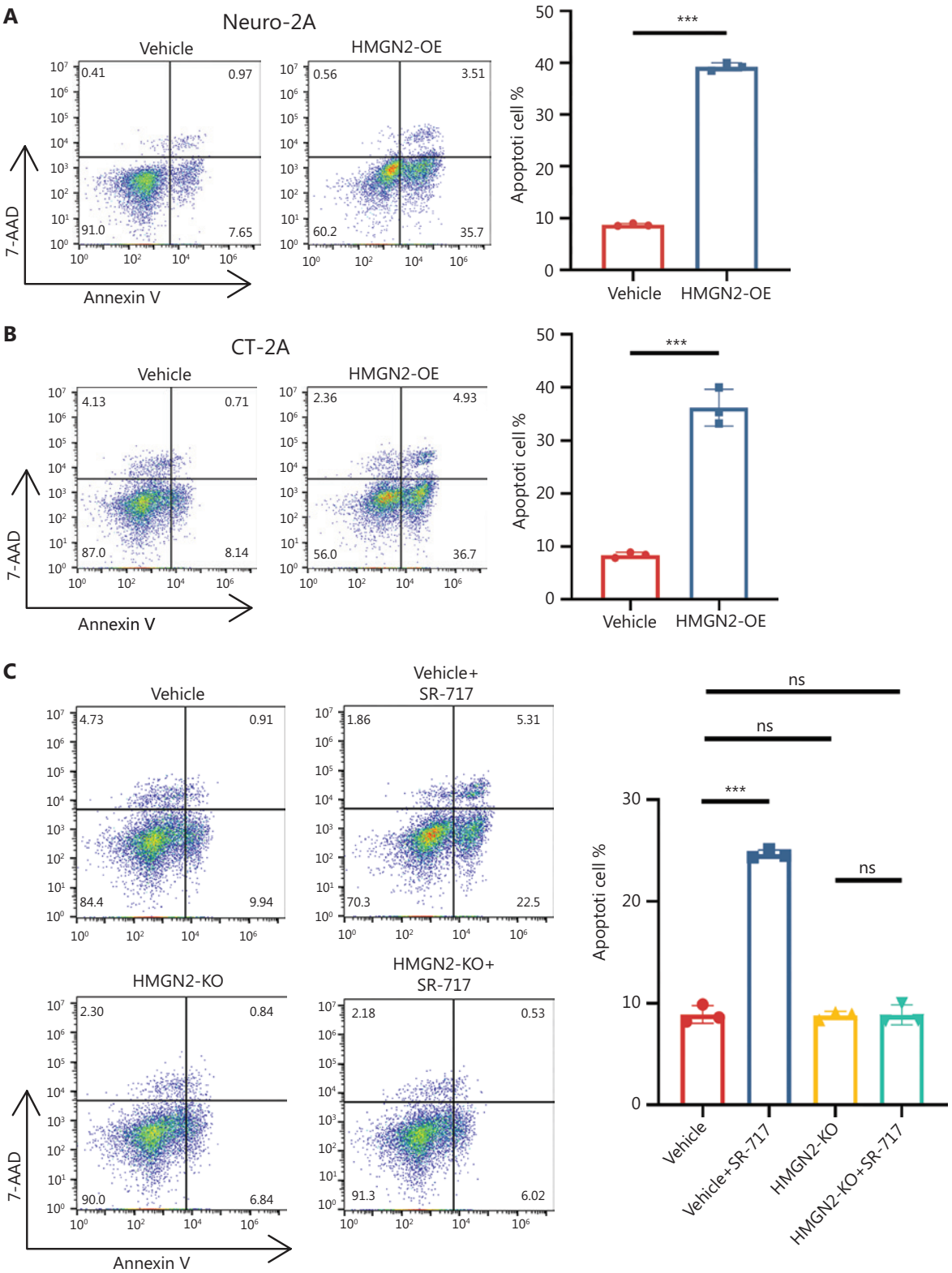


Figure 2 Continued

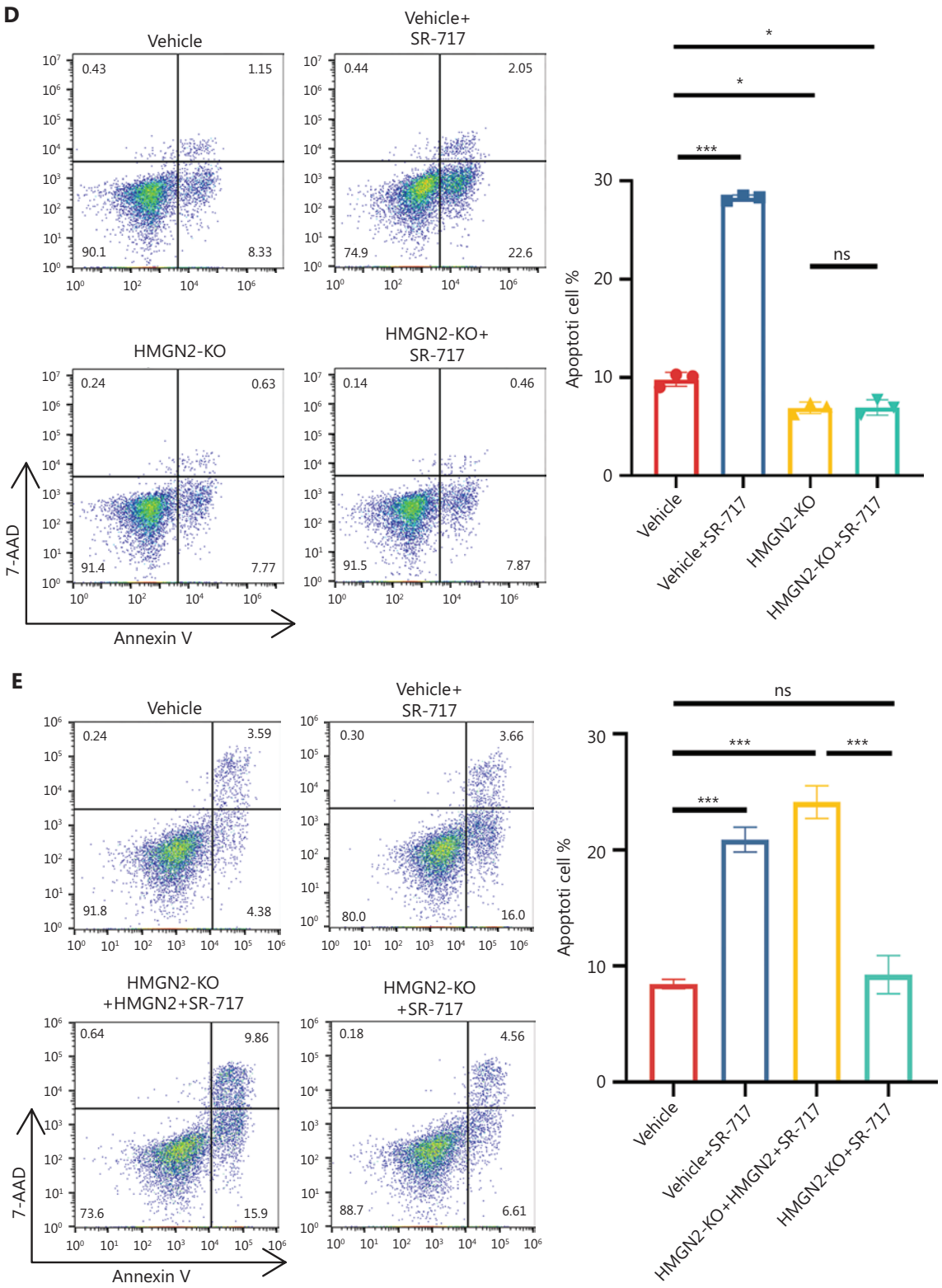


Figure 2 Continued

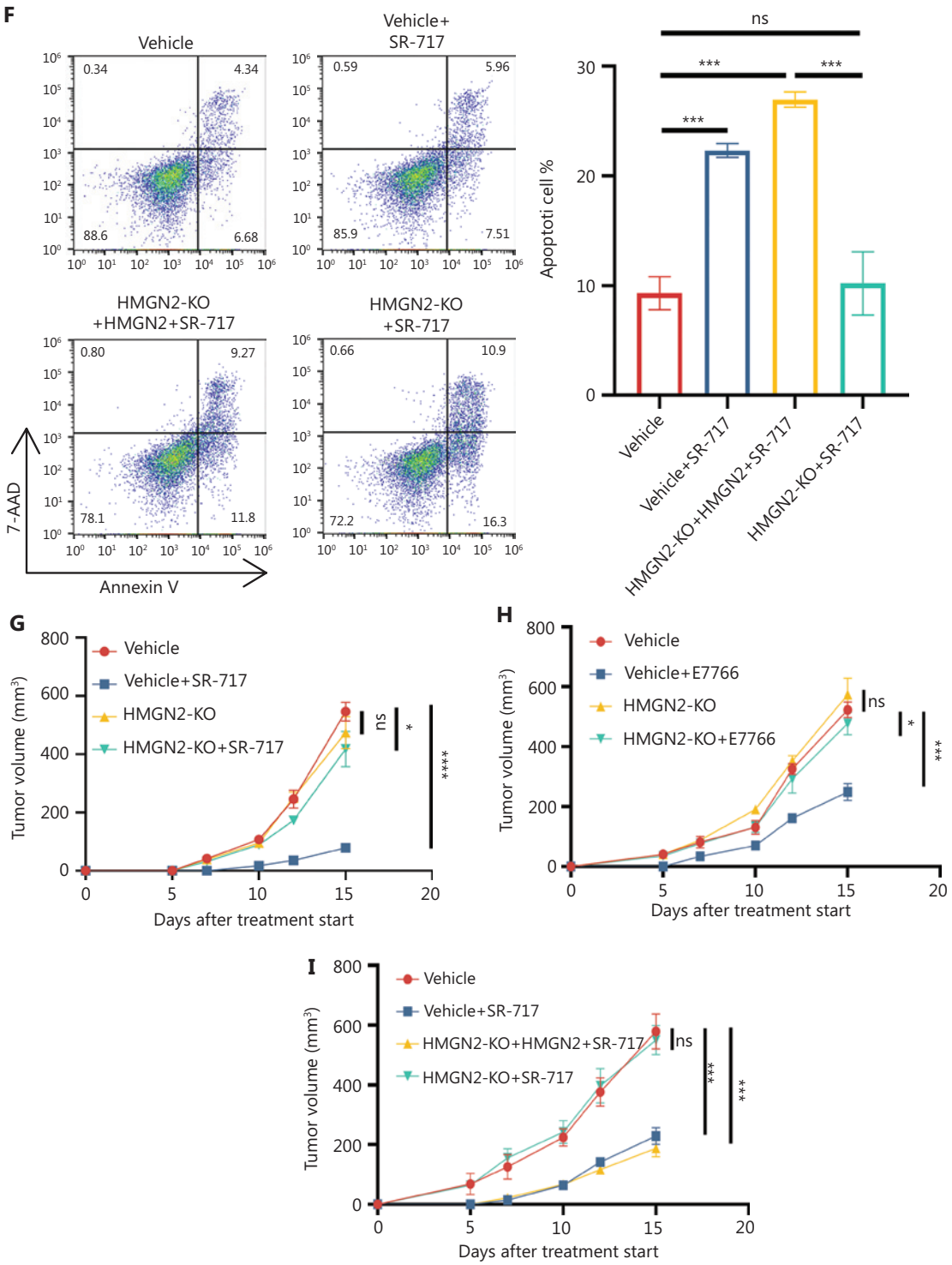


Figure 2 STING agonists mediate apoptosis in nervous system tumors *via HMGN2* upregulation. (A) FACS analysis of apoptosis levels in Neuro-2A cells with vehicle and HMGN2 overexpression. (B) FACS analysis of apoptosis levels in CT-2A cells with vehicle and HMGN2 overexpression. (C) FACS analysis of apoptosis levels in Neuro-2A cells treated with vehicle, vehicle+SR-717, HMGN2-KO, and HMGN2-KO+SR-717. (D) FACS analysis of apoptosis levels in CT-2A cells treated with vehicle, vehicle+SR-717, HMGN2-KO, and HMGN2-KO+SR-717. (E) FACS analysis of apoptosis levels in Neuro-2A cells treated with vehicle, vehicle+SR-717, HMGN2-KO+HMGN2+SR-717, and HMGN2-KO+SR-717. (F) FACS analysis of apoptosis levels in CT-2A cells treated with vehicle, vehicle+SR-717, HMGN2-KO+HMGN2+SR-717, and HMGN2-KO+SR-717. (G) Quantification of Neuro-2A tumor volume on the indicated days after the mice were treated with vehicle, vehicle+SR-717,

HMGN2-KO, and HMGN2-KO+SR-717 (n = 5). (H) Quantification of Neuro-2A tumor volume on the indicated days after the mice were treated with vehicle, vehicle+E7766, HMGN2-KO, and HMGN2-KO+E7766 (n = 5). (I) Quantification of Neuro-2A tumor volume on the indicated days after the mice were treated with vehicle, vehicle+SR-717, HMGN2-KO+SR-717, and HMGN2-KO+HMGN2+SR-717 (n = 5). The bars represent the mean ± S.D. (ns represents non-significant differences between the vehicle and HMGN2-KO+SR-717 groups, ***P < 0.001 for the difference between the vehicle and vehicle+SR-717 groups, and between the vehicle and HMGN2-KO+HMGN2+SR-717 groups, as determined by ANOVA with Tukey's honestly significant difference test for multiple comparisons). (ns, 0.05, *P < 0.05, ***P < 0.001, ****P < 0.0001, as determined by ANOVA with Tukey's honestly significant difference test for multiple comparisons). Vehicle group was treated with empty vector, HMGN2-OE group was treated with HMGN2-overexpressing lentiviral vectors, Vehicle+SR-717 group was obtained by treating Vehicle group with SR-717, HMGN2-KO group was treated with HMGN2 knockout sgRNA/Cas9 expression plasmids, HMGN2-KO+SR-717 group was obtained by treating the HMGN2-KO group with SR-717, HMGN2-KO+HMGN2+SR-717 group was established by performing HMGN2 overexpression in the HMGN2-KO group, followed by treatment with SR-717, Vehicle+E7766 was obtained by treating Vehicle group with E7766, HMGN2-KO+E7766 was obtained by treating the HMGN2-KO group with E7766.

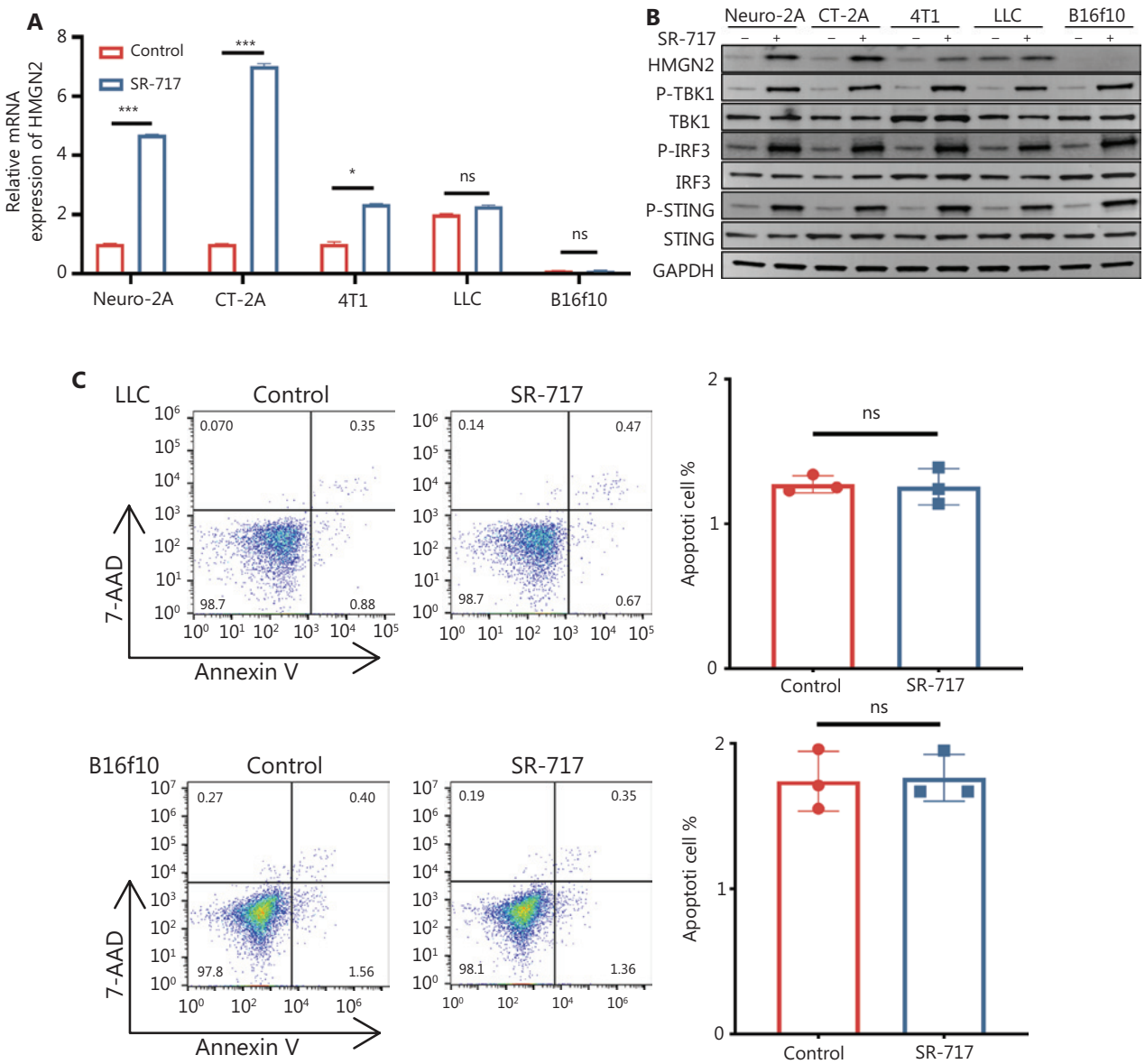


Figure 3 Continued

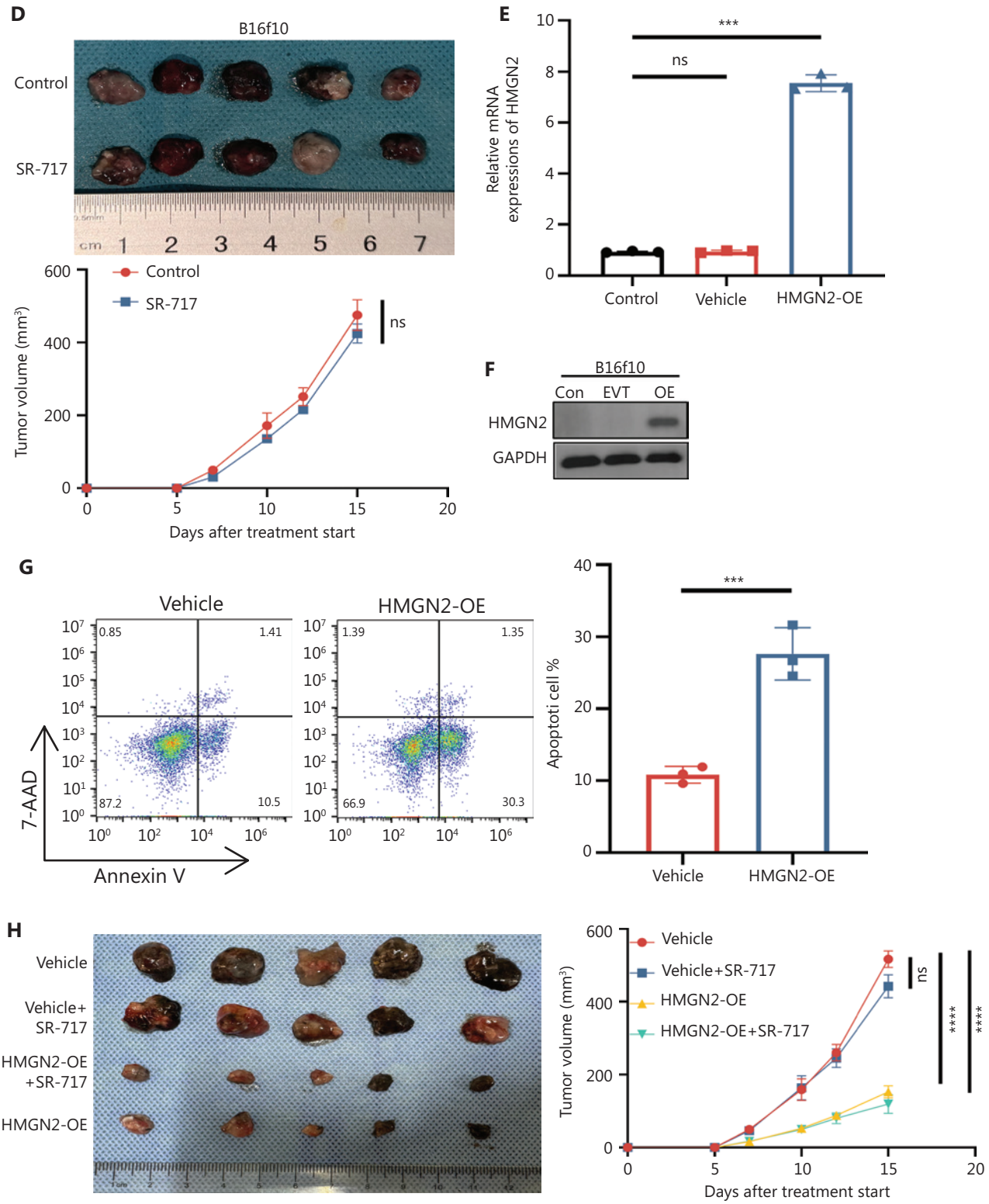


Figure 3 HMGN2 plays a crucial role in the antitumor effects of STING agonists. (A) RT-qPCR of HMGN2 in five cell types with or without SR-717 treatment. (B) Western blot of STING pathway and HMGN2 expression in five cell types upon SR-717 treatment. (C) FACS analysis of apoptosis levels in LLC and B16f10 cells upon control and SR-717 treatment. (D) Images of tumors in the B16f10 cell subcutaneous models; quantification of tumor volume on the indicated days after the mice were treated with SR-717 at a dose of 30 mg/kg (n = 5). (E) RT-qPCR

analysis of *HMGN2* gene mRNA levels in B16f10 cells after SR-717 treatment. (F) Western blot of HMGN2 overexpression in B16f10 cells. (G) FACS analysis of apoptosis levels in B16f10 cells upon vehicle and HMGN2 overexpression. (H) Images of tumors in the B16f10 cells subcutaneous model; quantification of tumor volume on the indicated days after the mice were treated with vehicle, vehicle+SR-717, HMGN2-OE, and HMGN2-OE+SR-717 (n = 5). The bars represent the mean ± S.D. (ns, 0.05, *P < 0.05, ***P < 0.001, ****P < 0.0001, as determined by ANOVA with Tukey's honestly significant difference test for multiple comparisons). Control group was untreated, SR-717 group was treated with SR-717, Vehicle group was treated with empty vector, HMGN2-OE group was treated with HMGN2-overexpressing lentiviral vectors, EVT group was treated with empty vector, OE group was treated with HMGN2-overexpressing lentiviral vectors, Vehicle+SR-717 group was obtained by treating Vehicle group with SR-717, HMGN2-OE+SR-717 group was obtained by treating HMGN2-OE group with SR-717.

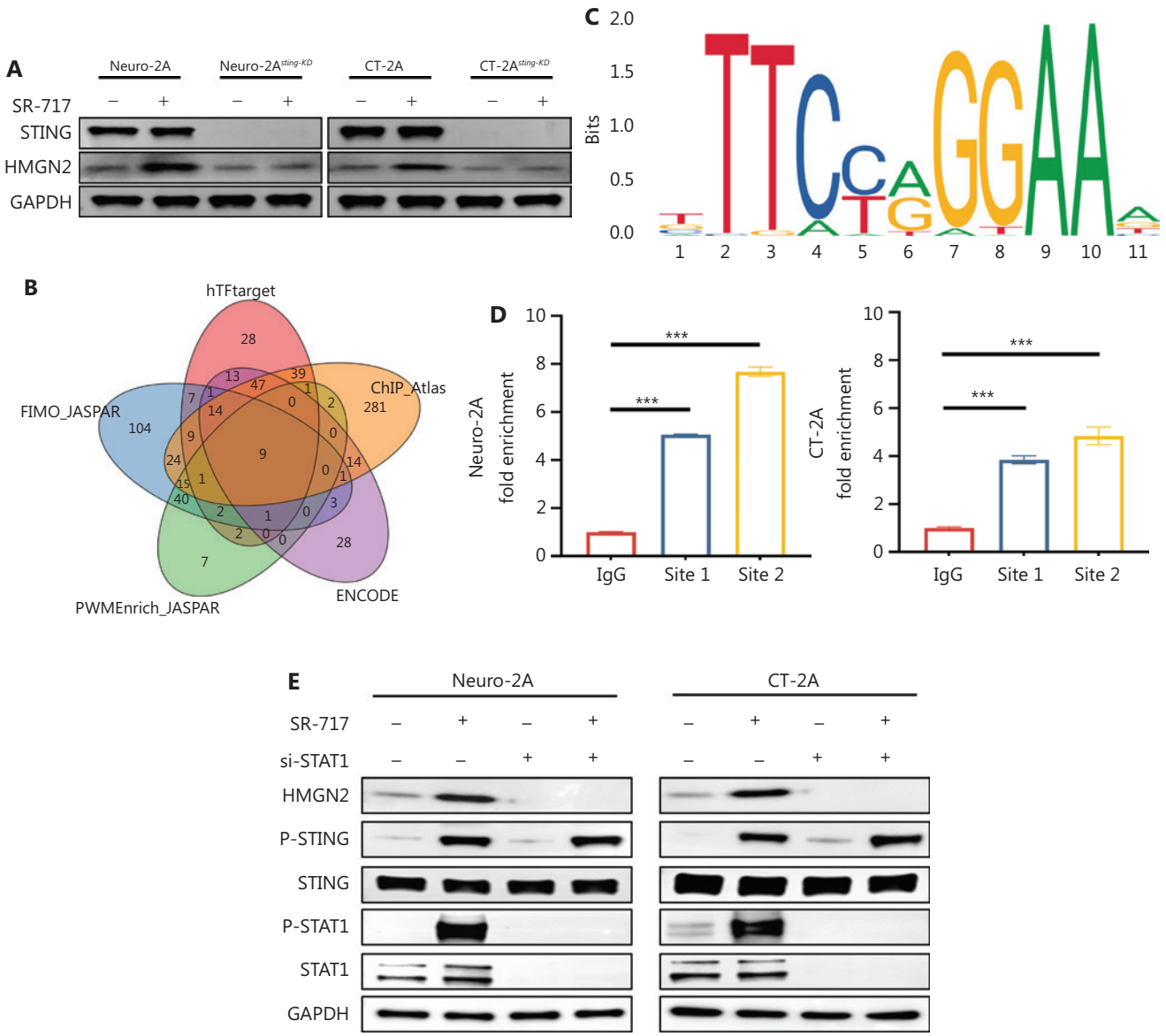


Figure 4 Continued

NSG mice implanted with HMGN2-overexpressing B16F10 cells exhibited significantly suppressed tumor growth. Notably, SR-717 treatment further enhanced tumor suppression, possibly by improving macrophage activity, which was consistent with previous results in Neuro-2A and CT-2A tumor models (**Figure 3H**).

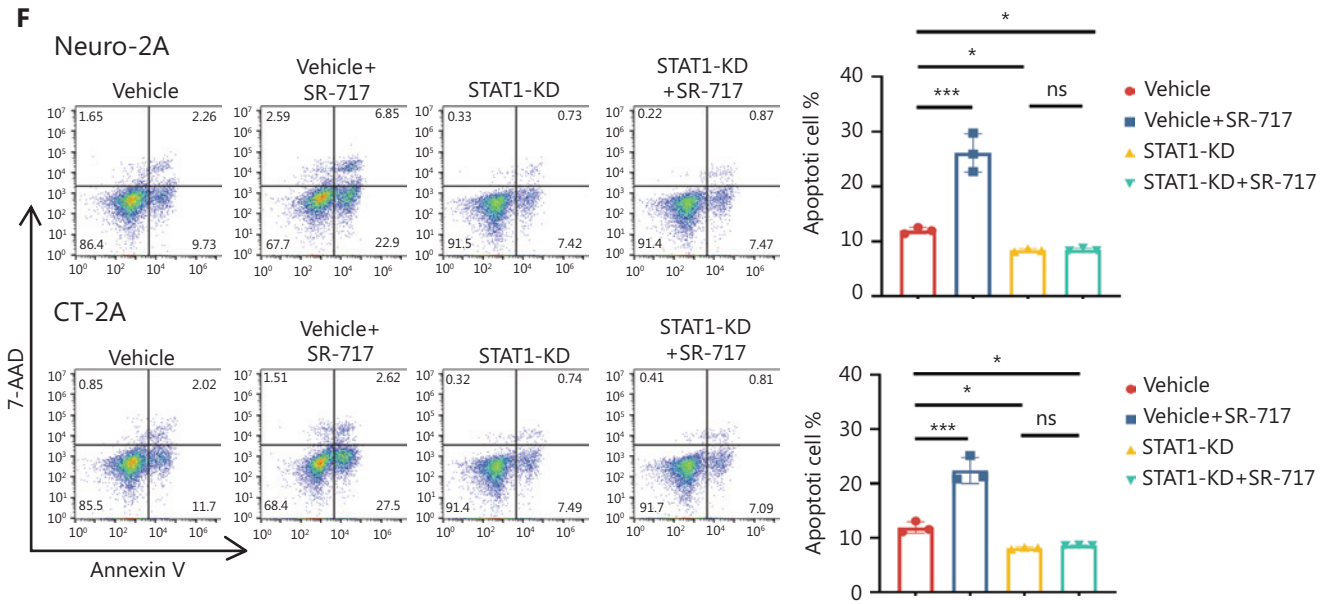


Figure 4 STING agonists upregulated HMGN2 *via* STAT1. (A) Western blot of STING and HMGN2 expression in Neuro-2A, Neuro-2A$^{sting\text{-}KD}$, CT-2A, and CT-2A$^{sting\text{-}KD}$ cells with or without SR-717 treatment. (B) HMGN2 upstream transcription factors prediction based on five databases. (C) Transcription factor binding sites were predicted using JASPAR databases. (D) ChIP-qPCR was used to detect the binding of STAT1 to the HMGN2 promoter in Neuro-2A and CT-2A cells. IgG was applied as a negative control. (E) Western blot analysis of HMGN2, p-STING, STING, p-STAT1, and STAT1 proteins in Neuro-2A and CT-2A cells treated with vehicle, vehicle+SR-717, si-STAT1, or si-STAT1+SR-717. (F) FACS analysis of apoptosis levels in Neuro-2A and CT-2A cells treated with vehicle, vehicle+SR-717, STAT1-KD, and STAT1-KD+SR-717. The bars represent the mean ± S.D. of triplicates. (ns, 0.05, *P < 0.05, ***P < 0.001, as determined by ANOVA with Tukey's honestly significant difference test for multiple comparisons). Control group was untreated, SR-717 group was treated with SR-717, igG group was non-specific IgG (negative control), Site 1 group was target site Site 1, Site 2 group was target site Site 2, Vehicle group was treated with empty interfering RNA, Vehicle+SR-717 group was obtained by treating Vehicle group with SR-717, STAT1-KD group was treated with interfering RNA, STAT1-KD+SR-717 group was obtained by treating the STAT1-KD group with SR-717.

Collectively, these findings identified HMGN2 as a critical mediator of STING agonist-induced tumor suppression.

STING agonists upregulate HMGN2 *via* STAT1

The precise mechanism underlying STING pathway-mediated regulation of HMGN2 expression has not been established. STING knockdown experiments were performed in Neuro-2A and CT-2A cells to clarify the mechanism (**Figure S4A**), followed by SR-717 treatment. Genetic deletion of STING completely abolished SR-717-induced HMGN2 upregulation, confirming direct regulation of HMGN2 expression by the STING pathway (**Figure 4A**).

Bioinformatics analyses were performed to identify potential regulators of HMGN2 given the involvement of multiple transcription factors downstream of STING (**Figure 4B**). Intersection analysis identified STAT1 as the most probable transcription factor regulating HMGN2. Further analysis using the JASPAR database predicted multiple STAT1-binding sites within the HMGN2 promoter (**Figures 4C and S4B**), suggesting transcriptional regulation by STAT1. In addition, previous studies by Du et al. confirmed that STAT1 in nervous system tumors is regulated through the cGAS-STING-type I interferon signaling axis[34].

Subsequent experiments were performed to verify whether STAT1 directly binds to the HMGN2 promoter to regulate transcription. ChIP-qPCR analysis demonstrated STAT1 binding to multiple sites in the HMGN2 promoter region (**Figure 4D**). In addition, STING agonist treatment elevated phosphorylated STAT1 levels, corresponding to increased HMGN2 expression. Conversely, STAT1 KO markedly decreased HMGN2 expression (**Figures 4E and S4C–E**). These findings support a model in which STAT1 mediates HMGN2 expression downstream of STING activation.

Flow cytometry analysis was performed to confirm the functional importance of the STING-STAT1-HMGN2 axis in apoptosis induction in neural tumor cells (**Figure 4F**). STAT1 KO significantly reduced STING-induced apoptosis. This finding validated the critical role of STAT1 in apoptosis mediated by the STING signaling pathway and highlighted the

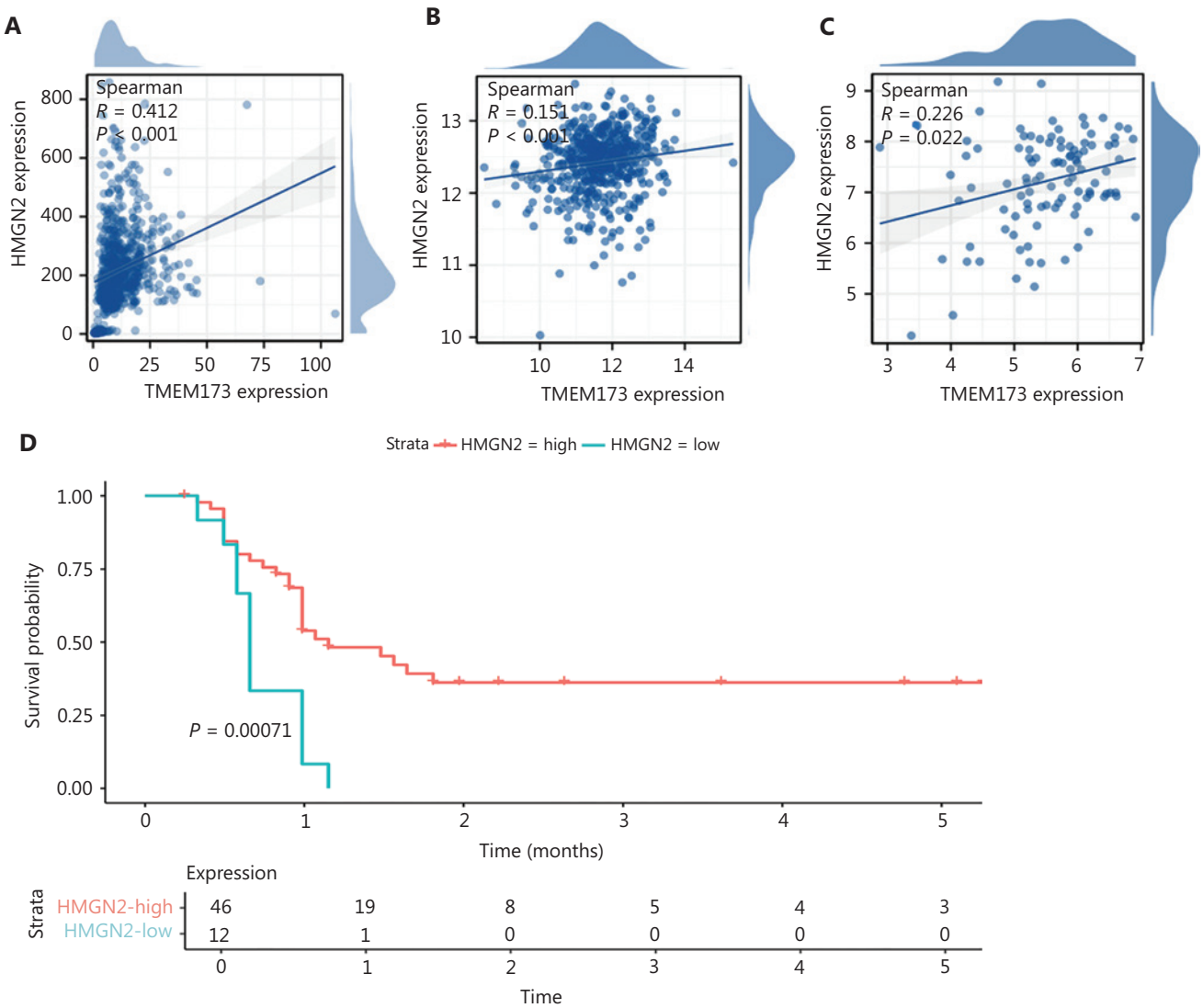


Figure 5 Continued

functional importance of the STING-STAT1-HMGN2 axis in nervous system tumors.

Taken together, activation of STING signaling in nervous system tumor cells induced apoptosis through the STAT1-mediated upregulation of HMGN2.

HMGN2 expression correlates with survival in multiple malignancies

To explore clinical relevance, public databases were analyzed to determine associations between STING and HMGN2 expression. Analysis of public data for GBM, NB, and melanoma revealed significant correlations between STING and HMGN2 transcript levels (**Figure 5A–C**). Furthermore, survival analysis using data from TCGA indicated that elevated HMGN2 expression correlated positively with better patient outcomes in NB and GBM (**Figure 5D,E**). This positive correlation extended to melanoma, in which high HMGN2 expression was associated with superior patient survival (**Figure 5F**). However, the lack of anti-tumor efficacy observed in the B16F10 murine melanoma model might be attributed to species-specific differences in HMGN2 expression between murine and human melanoma cells.

Analyses were expanded to include pancreatic cancer, colorectal cancer, cervical cancer, and clear cell renal carcinoma to test the broader applicability of this observation. Consistently, high HMGN2 expression correlated with improved survival across these cancer types (**Figure 5G–J**).

In summary, HMGN2 expression was shown to be significantly correlated with STING expression and may serve as a

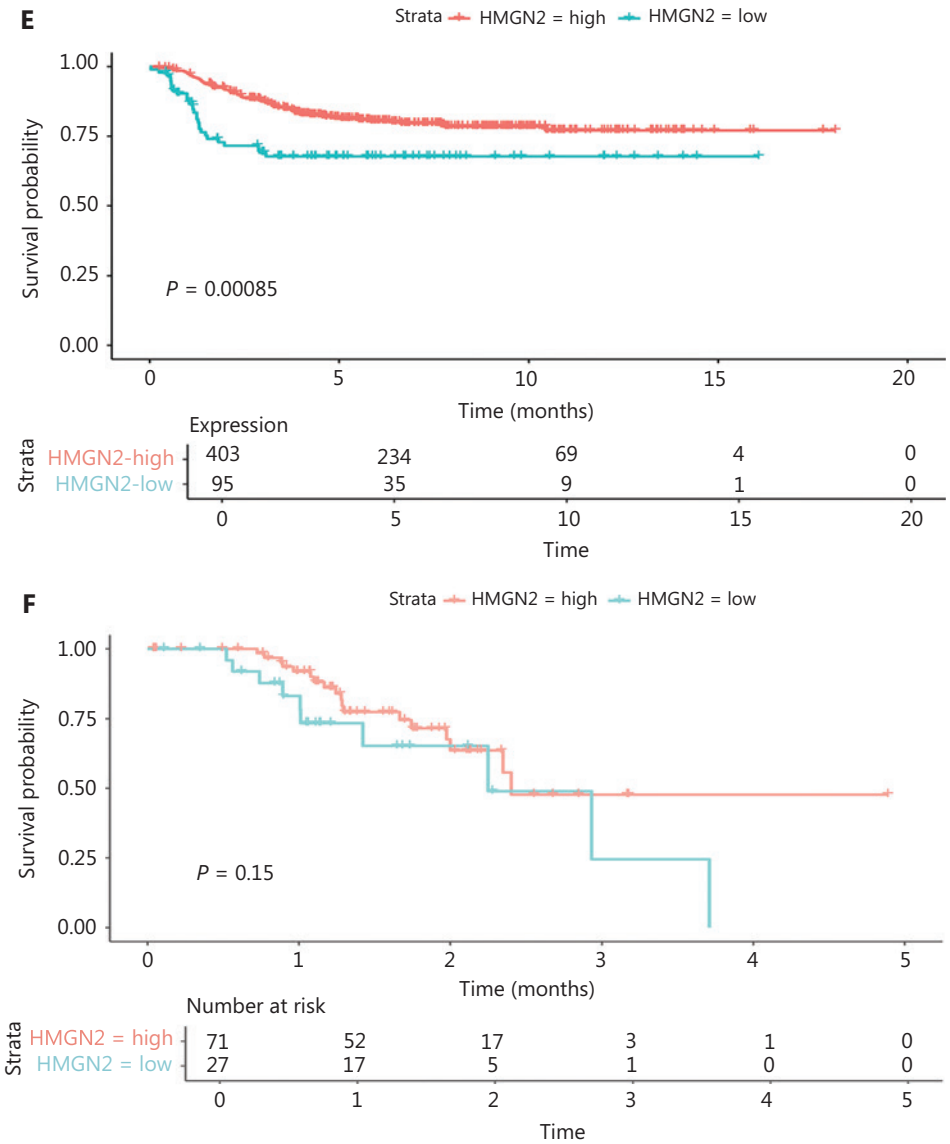


Figure 5 Continued

predictive biomarker for STING agonist efficacy. Patients with elevated HMGN2 expression are likely to benefit substantially from STING agonist therapies, leading to improved survival outcomes.

Discussion

As promising candidates for cancer immunotherapy, the clinical translation of STING agonists has been limited by restricted efficacy and potential pro-tumorigenic effects observed in certain models[35-37]. Therefore, identifying tumor types sensitive to STING agonists and clarifying the underlying mechanisms is essential to facilitate clinical application[38,39]. This is the first study to show that the STING agonist, SR-717, exhibits distinct antitumor activity against nervous system tumors, including NB and GBM. Although minimal differences were observed in cell-based assays, parallel *in vivo* comparisons using mouse models showed that the non-nucleotide agonist, SR-717, had superior antitumor efficacy compared to the macrocyclic agonist, E7766. This enhanced efficacy primarily depended on activation of the intrinsic STING signaling pathway within tumor cells, not solely the previously recognized activation of innate immune cells, resulting in increased expression of the novel downstream target, HMGN2, and subsequent induction of apoptosis.

Currently, effective treatments for NB and GBM remain inadequate, primarily due to the unique immunosuppressive microenvironment[40]. This microenvironment, dominated by myeloid cells and characterized by limited lymphocyte

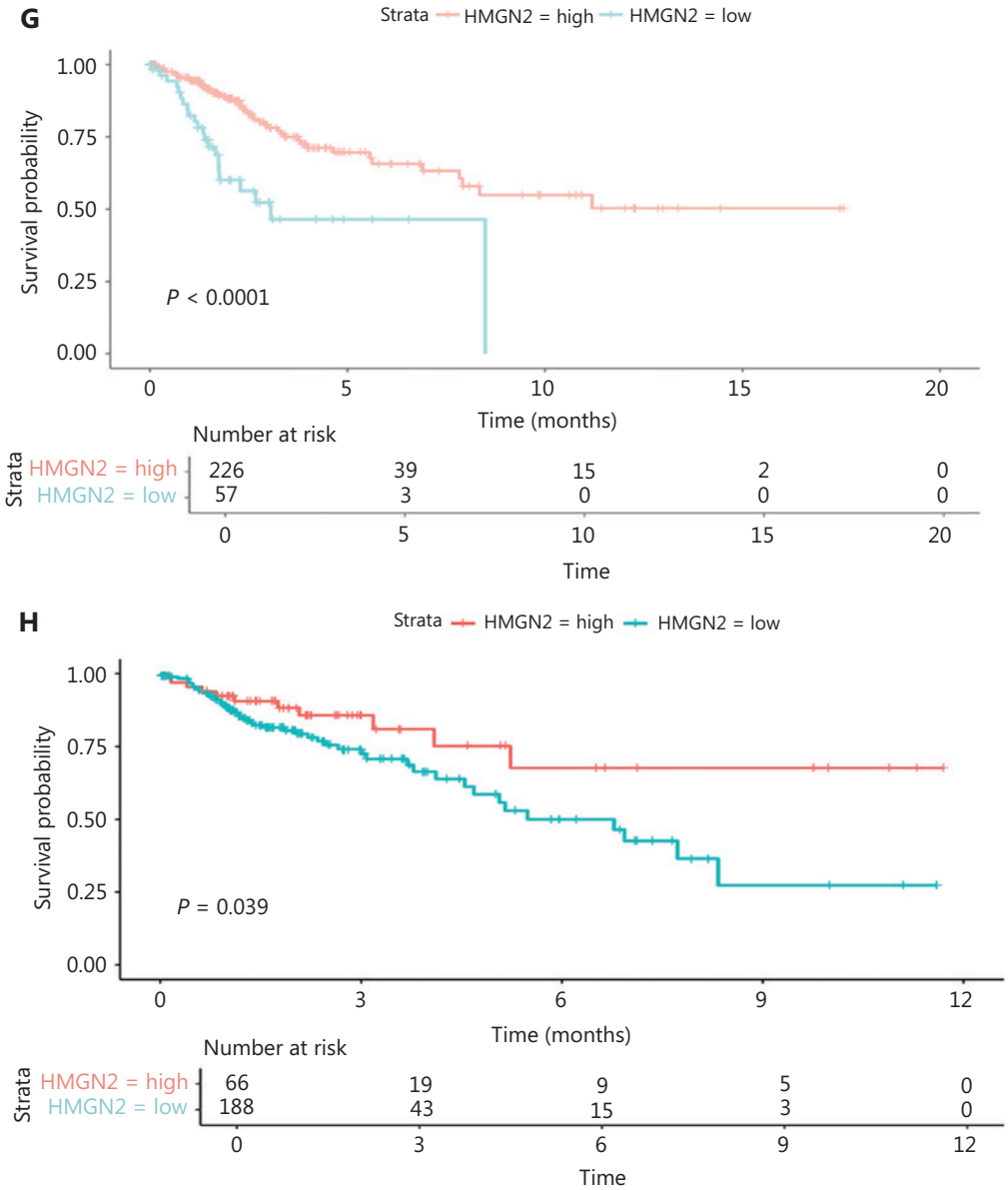


Figure 5 Continued

infiltration, renders conventional immunotherapies largely ineffective. This observation prompted the exploration of therapeutic approaches directly targeting tumor cells. Validation using mouse models with different degrees of immunodeficiency ($Rag^{-/-}$ and NSG mice) confirmed that the direct cytotoxic effects of SR-717 on nervous system tumors were independent of adaptive immune responses. However, the more pronounced efficacy observed in immunocompetent mice indicated that an intact immune might provide an important supportive role, potentially through residual macrophages that clear apoptotic cells and release inflammatory factors. This finding suggested a rationale for future combination immunotherapy.

Mechanistically, a major breakthrough of this study was the identification of HMGN2 as a novel direct downstream target of the STING signaling pathway. Functional experiments demonstrated that elevated HMGN2 expression was sufficient to induce tumor cell apoptosis. In addition, HMGN2 expression induced by STING activation in nervous system tumor cells (Neuro-2A and CT-2A) strictly depended on the presence of the STING protein. Further analysis uncovered a non-canonical STING signaling pathway: STING activation directly regulated HMGN2 transcription *via* STAT1 rather than solely through the Interferon Regulatory Factor 3 (IRF3)/IFN axis, thereby enhancing caspase-3 cleavage and apoptosis. This newly identified STING-STAT1-HMGN2

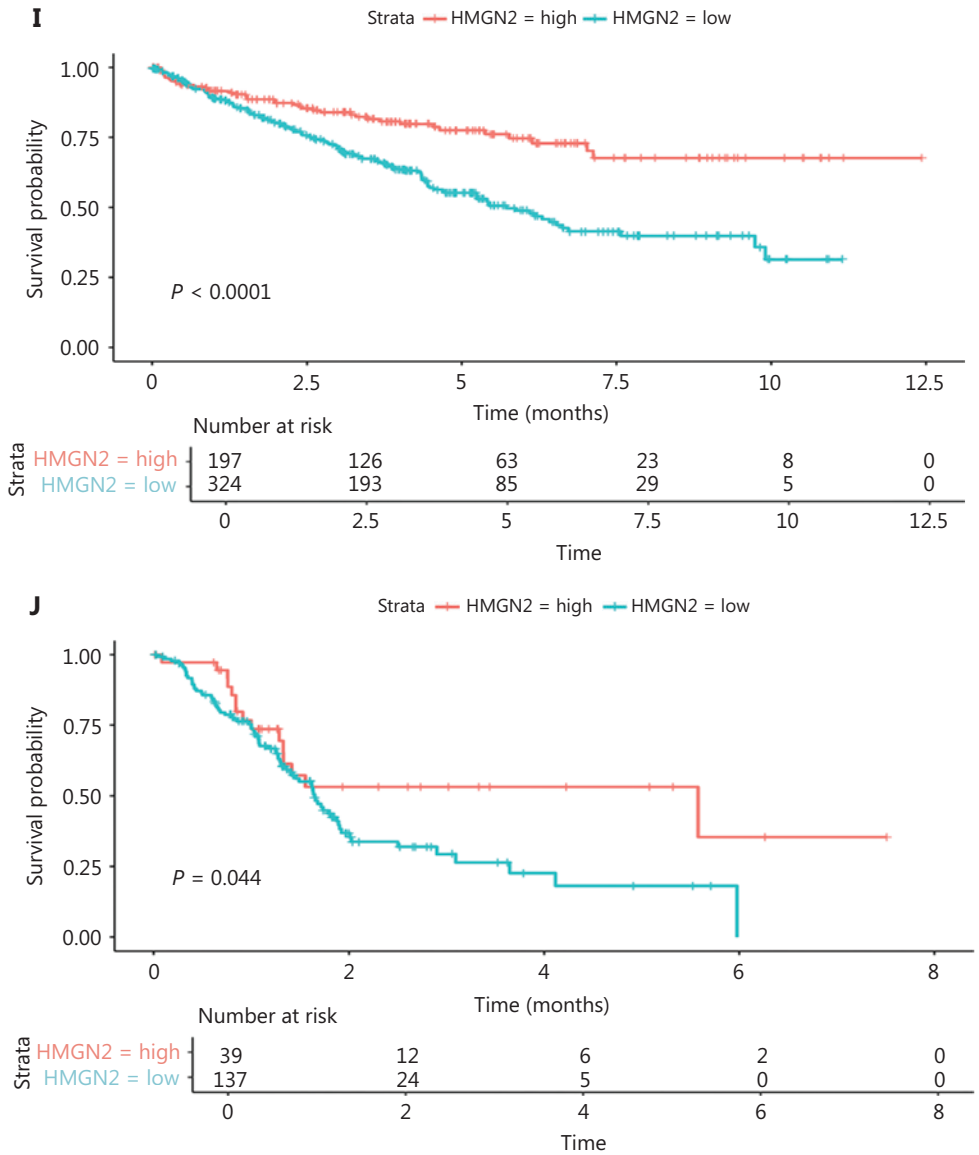


Figure 5 HMGN2 expression correlates with survival in multiple malignancies. (A) Spearman correlation between expression of HMGN2 and TMEM173 (STING) in the GEO neuroblastoma cancer data. (B) Spearman correlation between expression of HMGN2 and TMEM173 (STING) in the TCGA glioblastoma data. (C) Spearman correlation between expression of HMGN2 and TMEM173 (STING) in the TCGA melanoma data. (D) KM survival curve based on HMGN2 expression using TCGA neuroblastoma cancer data. (E) KM survival curve based on HMGN2 expression using TCGA glioblastoma data. (F) KM survival curve based on HMGN2 expression using TCGA melanoma data. (G) KM survival curve based on HMGN2 expression using TCGA pancreatic cancer data. (H) KM survival curve based on HMGN2 expression using TCGA colon cancer data. (I) KM survival curve based on HMGN2 expression using TCGA cervical cancer data. (J) KM survival curve based on HMGN2 expression using TCGA clear cell renal cell carcinoma data.

axis provides critical insight into the molecular mechanism by which STING agonists induce direct tumor-cell apoptosis and expands the current understanding of STING biology by identifying potential targets for developing novel therapeutic strategies against nervous system tumors (**Figure 6**).

Another significant implication of this study was the identification of HMGN2 as a potential prognostic biomarker. HMGN2 expression was less influenced by immune cell infiltration within the tumor microenvironment compared to IFN-β and is predominantly regulated by the intrinsic STING/STAT1 pathway within tumor cells. Therefore, HMGN2 may reflect apoptotic potential and tumor malignancy more accurately and specifically, potentially improving prognostic assessments for nervous system tumors. However, further

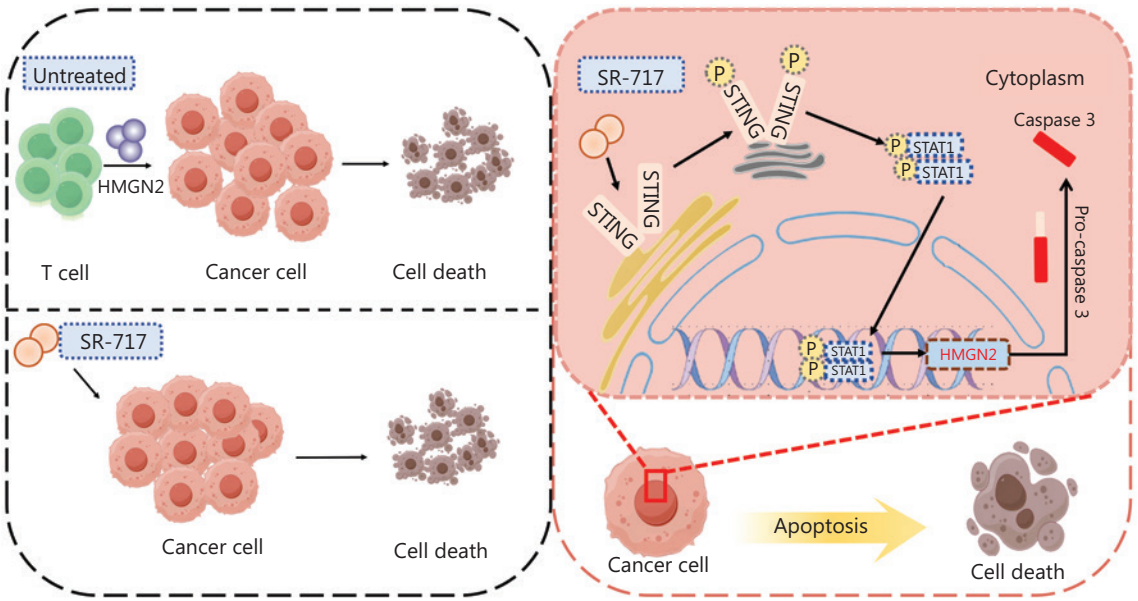


Figure 6 Mechanism of SR-717-induced apoptosis in nervous system tumors. SR-717 is a novel non-nucleotide STING agonist. Before treatment (upper left panel) only a small subset of activated T cells within the tumor microenvironment secreted limited amounts of HMGN2, resulting in minimal tumor cell apoptosis. After intratumoral SR-717 administration (lower left panel) HMGN2 expression in tumor cells significantly increased, directly inducing apoptosis. Specifically, SR-717 activates the intrinsic STING signaling pathway within tumor cells (right panel). Activated STING promotes phosphorylation of STAT1, which subsequently translocate into the nucleus and enhances transcription of HMGN2. Increased HMGN2 expression facilitates caspase-3 cleavage, ultimately triggers apoptosis. Therefore, SR-717 induces apoptosis by activating the tumor-intrinsic STING-STAT1-HMGN2 signaling axis. This finding expands the mechanistic understanding of STING agonists and highlights the therapeutic potential in clinical applications. HMGN2, high-mobility group nucleosome-binding domain 2; STING, stimulator of interferon genes; STAT1, signal transducer and activator of transcription 1.

validation in large-scale clinical cohorts is necessary, particularly through direct comparisons with established biomarkers, such as IFN-β.

Based on these findings, future research can be expanded in two directions: 1) exploring combination therapies given that SR-717 directly induces tumor cell death and potentially modifies the tumor microenvironment. For instance, combining SR-717 with immune checkpoint inhibitors (PD-1/PD-L1 blockers) may yield synergistic effects of direct tumor killing and immune suppression reversal, which is especially suitable for immunologically "cold" nervous system tumors; 2) developing targeted drug-delivery systems to overcome issues associated with systemic administration of STING agonists, such as rapid metabolism and insufficient targeting. Delivering systems utilizing nanotechnology or tumor-specific antigens can enhance SR-717 accumulation at tumor sites, improving therapeutic efficacy, minimizing systemic toxicity, and accelerating clinical translation.

Conclusions

Overall, the current study demonstrated that STING agonists can induce tumor cell apoptosis *via* activating the STING-STAT1-HMGN2 signaling pathway, thereby exerting a potent antitumor effect in nervous system tumors. *In vivo* experiments further confirmed that the therapeutic efficacy of SR-717 is significantly superior to E7766. In addition, HMGN2 may serve as a prognostic biomarker for predicting patient survival outcomes, with extremely high translational application value.

Conflict of interest statement

No potential conflicts of interest are disclosed.

Author contributions

Conceived and designed the analysis: Weidong Han, Qian Mei, Zhengfan Jiang and Zijian Lv.
Performed the experiments: Zijian Lv, Tiance Wang, Runjia Fan and Qianyi Ming.
Assisted in the experiments: Jiejie Liu, Yulin Jia, Yan Zhang, Meixia Chen and Wei Chen.
Performed the analysis: Zijian Lv, Tiance Wang.
Wrote the paper: Zijian Lv, Tiance Wang.

Data availability statement

Data supporting the findings of this study are available from the corresponding author upon reasonable request.

References

1. Wang R, Lan C, Benlagha K, Camara NOS, Miller H, Kubo M, et al. The interaction of innate immune and adaptive immune system. MedComm (2020). 2024; 5: e714.
2. Sun L, Wu J, Du F, Chen X, Chen ZJ. Cyclic GMP-AMP synthase is a cytosolic DNA sensor that activates the type I interferon pathway. Science. 2013; 339: 786-91.
3. Woo SR, Fuertes MB, Corrales L, Spranger S, Furdyna MJ, Leung MY, et al. STING-dependent cytosolic DNA sensing mediates innate immune recognition of immunogenic tumors. Immunity. 2014; 41: 830-42.
4. Chen Q, Sun L, Chen ZJ. Regulation and function of the cGAS-STING pathway of cytosolic DNA sensing. Nat Immunol. 2016; 17: 1142-9.
5. Woo SR, Corrales L, Gajewski TF. The STING pathway and the T cell-inflamed tumor microenvironment. Trends Immunol. 2015; 36: 250-6.
6. Deng L, Liang H, Xu M, Yang X, Burnette B, Arina A, et al. STING-dependent cytosolic DNA sensing promotes radiation-induced type I interferon-dependent antitumor immunity in immunogenic tumors. Immunity. 2014; 41: 843-52.
7. Dou Z, Ghosh K, Vizioli MG, Zhu J, Sen P, Wangensteen KJ, et al. Cytoplasmic chromatin triggers inflammation in senescence and cancer. Nature. 2017; 550: 402-6.
8. Ishikawa H, Ma Z, Barber GN. STING regulates intracellular DNA-mediated, type I interferon-dependent innate immunity. Nature. 2009; 461: 788-92.
9. Mackenzie KJ, Carroll P, Martin CA, Murina O, Fluteau A, Simpson DJ, et al. cGAS surveillance of micronuclei links genome instability to innate immunity. Nature. 2017; 548: 461-5.
10. Xu MM, Pu Y, Han D, Shi Y, Cao X, Liang H, et al. Dendritic cells but not macrophages sense tumor mitochondrial DNA for cross-priming through signal regulatory protein α signaling. Immunity. 2017; 47: 363-73.e5.
11. Yang Y, Wu M, Cao D, Yang C, Jin J, Wu L, et al. ZBP1-MLKL necroptotic signaling potentiates radiation-induced antitumor immunity via intratumoral STING pathway activation. Sci Adv. 2021; 7: eabf6290.
12. Hemann EA, Green R, Turnbull JB, Langlois RA, Savan R, Gale M Jr. Interferon-λ modulates dendritic cells to facilitate T cell immunity during infection with influenza A virus. Nat Immunol. 2019; 20: 1035-45.
13. Wang Y, Luo J, Alu A, Han X, Wei Y, Wei X. cGAS-STING pathway in cancer biotherapy. Mol Cancer. 2020; 19: 136.
14. Fan JB, Miyauchi S, Xu HZ, Liu D, Kim LJY, Burkart C, et al. Type I interferon regulates a coordinated gene network to enhance cytotoxic T cell-mediated tumor killing. Cancer Discov. 2020; 10: 382-93.
15. Schmid M, Fischer P, Engl M, Widder J, Kerschbaum-Gruber S, Slade D. The interplay between autophagy and cGAS-STING signaling and its implications for cancer. Front Immunol. 2024; 15: 1356369.
16. Jiang M, Chen P, Wang L, Li W, Chen B, Liu Y, et al. cGAS-STING, an important pathway in cancer immunotherapy. J Hematol Oncol. 2020; 13: 81.
17. Ochoa de Olza M, Oliva M, Hierro C, Matos I, Martin-Liberal J, Garralda E. Early-drug development in the era of immuno-oncology: are we ready to face the challenges? Ann Oncol. 2018; 29: 1727-40.
18. Ying X, Chen Q, Yang Y, Wu Z, Zeng W, Miao C, et al. Nanomedicines harnessing cGAS-STING pathway: sparking immune revitalization to transform 'cold' tumors into 'hot' tumors. Mol Cancer. 2024; 23: 277.
19. Gehrcken L, Deben C, Smits E, Van Audenaerde JRM. STING agonists and how to reach their full potential in cancer immunotherapy. Adv Sci (Weinh). 2025; 12: e2500296.
20. Vitale I, Shema E, Loi S, Galluzzi L. Intratumoral heterogeneity in cancer progression and response to immunotherapy. Nat Med. 2021; 27: 212-24.
21. Lim ZF, Ma PC. Emerging insights of tumor heterogeneity and drug resistance mechanisms in lung cancer targeted therapy. J Hematol Oncol. 2019; 12: 134.
22. Ohkuri T, Ghosh A, Kosaka A, Zhu J, Ikeura M, David M, et al. STING contributes to antiglioma immunity via triggering type I IFN signals in the tumor microenvironment. Cancer Immunol Res. 2014; 2: 1199-208.
23. Zhang H, Wang Z, Wu J, Zheng YQ, Zhao Q, He S, et al. Endothelial STING-JAK1 interaction promotes tumor vasculature normalization and antitumor immunity. J Clin Invest. 2025; 135: e180622.
24. Zhu Y, An X, Zhang X, Qiao Y, Zheng T, Li X. STING: a master regulator in the cancer-immunity cycle. Mol Cancer. 2019; 18: 152.
25. Low JT, Brown MC, Reitman ZJ, Bernstock JD, Markert JM, Friedman GK, et al. Understanding and therapeutically exploiting cGAS/STING signaling in glioblastoma. J Clin Invest. 2024; 134: e163452.
26. Liu J, Zhou J, Luan Y, Li X, Meng X, Liao W, et al. cGAS-STING, inflammasomes and pyroptosis: an overview of crosstalk mechanism of activation and regulation. Cell Commun Signal. 2024; 22: 22.
27. Liu Y, Xu P, Rivara S, Liu C, Ricci J, Ren X, et al. Clathrin-associated AP-1 controls termination of STING signalling. Nature. 2022; 610: 761-7.
28. Martínez de Paz A, Ausió J. HMGNs: the enhancer charmers. Bioessays. 2016; 38: 226-31.
29. Li G, Zhang G, Li J, Zhang J, Yang Z, Yang L, et al. High mobility group protein N2 inhibits the progression of hepatocellular

carcinoma and the related molecular mechanisms. Cytotechnology. 2025; 77: 20.
30. Su L, Hu A, Luo Y, Zhou W, Zhang P, Feng Y. HMGN2, a new anti-tumor effector molecule of $CD8^+$ T cells. Mol Cancer. 2014; 13: 178.
31. Huang X, Huo L, Xiao B, Ouyang Y, Chen F, Li J, et al. Activating STING/TBK1 suppresses tumor growth via degrading HPV16/18 E7 oncoproteins in cervical cancer. Cell Death Differ. 2024; 31: 78-89.
32. Chin EN, Yu C, Vartabedian VF, Jia Y, Kumar M, Gamo AM, et al. Antitumor activity of a systemic STING-activating non-nucleotide cGAMP mimetic. Science. 2020; 369: 993-9.
33. Hildebrand KM, Hildebrand KN, Salazar Arcila C, Marritt K, Rajwani J, Elmi Assadzadeh G, et al. The human STING agonist E7766 induces immunogenic tumor clearance, independent of tumor-intrinsic STING expression in the $KRAS^{G12D/+}$ $Trp^{53-/-}$ murine model of sarcoma. Oncoimmunology. 2025; 14: 2534912.
34. Du J, Kageyama SI, Yamashita R, Hirata H, Hakozaki Y, Okumura M, et al. Impacts of the STING-IFNAR1-STAT1-IRF1 pathway on the cellular immune reaction induced by fractionated irradiation. Cancer Sci. 2022; 113: 1352-61.
35. Zhang J, Yu S, Peng Q, Wang P, Fang L. Emerging mechanisms and implications of cGAS-STING signaling in cancer immunotherapy strategies. Cancer Biol Med. 2024; 21: 45-64.
36. Hsu NS, Tang C, Mendes RV, Labão-Almeida C, Dos Reis CV, Coelho AR, et al. Tumour-specific STING agonist synthesis via a two-component prodrug system. Nat Chem. 2025.
37. Shen M, Jiang X, Peng Q, Oyang L, Ren Z, Wang J, et al. The cGAS–STING pathway in cancer immunity: mechanisms, challenges, and therapeutic implications. J Hematol Oncol. 2025; 18: 40.
38. Chamma H, Vila IK, Taffoni C, Turtoi A, Laguette N. Activation of STING in the pancreatic tumor microenvironment: a novel therapeutic opportunity. Cancer Lett. 2022; 538: 215694.
39. Wang B, Yu W, Jiang H, Meng X, Tang D, Liu D. Clinical applications of STING agonists in cancer immunotherapy: current progress and future prospects. Front Immunol. 2024; 15: 1485546.
40. Najem H, Lea ST, Tripathi S, Hurley L, Chen CH, William I, et al. STING agonist 8803 reprograms the immune microenvironment and increases survival in preclinical models of glioblastoma. J Clin Invest. 2024; 134: e175033.

Cite this article as: Lv Z, Wang T, Fan R, Ming Q, Liu J, Jia Y, et al. Antitumor effects of STING agonists on nervous system tumors *via* tumor-intrinsic STING-STAT1-mediated HMGN2 expression. Cancer Biol Med. 2026; 23: 133-153. doi: 10.20892/j.issn.2095-3941.2025.0326